DOE/ET-53088-252 IFSR #252

Papers presented by IFS/FRC members at The International Workshop on Small Scale Turbulence and Anomalous Transport in Magnetized Plasmas Cargese, Corsica (France), July 7–11, 1986

B. D. Scott, R. D. Bengtson, P. H. Diamond, and *P. W. Terry*

Institute for Fusion Studies
and
Fusion Research Center
The University of Texas
Austin, Texas 78712

September 1986

CONTENTS

Turbulent Drift-wave Dynamics and Coherent Structures

B. D. Scott, P. W. Terry, P. H. Diamond 1

Fluctuations and Transport Measurements in the TEXT Tokamak

Roger D. Bengtson, R. V. Bravenec, D. L. Brower, P. H. Diamond, K. W. Gentle, C. C. Klepper, N. C. Luhmann, Jr., W. A. Peebles, P. E. Phillips, E. J. Powers, T. L. Rhodes, B. Richards, Ch. P. Ritz, W. L. Rowan, A. J. Wootton 5

Ion Pressure Gradient Driven Turbulence: Theory and Consequences

P. H. Diamond, G. S. Lee, N. Mattor, P. T. Katt 20

Localized Fluctuations in Inhomogeneous Plasma Turbulence: Structure, Dynamics, Relaxation, and Transport

P. W. Terry, P. H. Diamond, T. S. Hahm 25

Turbulent Drift-wave Dynamics and Coherent Structures

Bruce D. Scott, P. W. Terry, and P. H. Diamond
Institute for Fusion Studies, University of Texas, Austin, TX 78712

ABSTRACT

The dynamics of decaying 2D drift-wave turbulence are investigated numerically in the absence of assumptions in the relation between the electrostatic potential and the density response, with the result that nonlinear coupling dominates this in the hydrodynamic region about the resonant surface. Outside this region, an adiabatic relation prevails. Thus, the nonadiabatic density response is small away from the resonant surface but can be as large as the potential fluctuation near it. This response is much more self-coherent than either the density or potential fluctuations and decays more slowly as well, becoming dominant.

I. Introduction

The electrostatic drift wave has for at least a decade been thought responsible in part, or in whole, for the anomalous transport of heat and particles in tokamak fusion devices.[1] Nonlinear drift-wave turbulence is essentially electrostatic $\mathbf{E} \times \mathbf{B}$ convective turbulence with the density gradient as a free energy source and with magnetic shear damping as the sink. Higher-order effects such as coupling to trapped electrons or toroidicity are necessary for the waves to be unstable. However, it is possible to study the essential physics of the fluctuations by investigating decaying nonlinear drift-wave turbulence in a slab model with shear.

Previous efforts have usually made use of the adiabatic assumption, in which electrostatic and internal energy in the fluctuations are equipartitioned by diffusive processes on a time scale fast compared to that of the waves, yielding the simplifying relation $\widetilde{n}/n_0 = e\widetilde{\phi}/T$.[2] The advantage of this is that without magnetic shear only one equation, the Hasegawa-Mima equation is needed to model the fluctuations. To provide for instability, and a cross-field particle flux, a small phase shift is introduced for each wave, so that in wavenumber space one has $\widetilde{n}_{\mathbf{k}}/n_0 = (e\widetilde{\phi}_{\mathbf{k}}/T)(1 - i\delta_{\mathbf{k}})$. This will be referred to as the "i-delta" treatment. Since for all but the smallest tokamaks the perpendicular diffusion time scale is slow compared to the diamagnetic time scale, ω_*^{-1}, the condition for adiabaticity is $k_\parallel^2 V_e^2 \gg \omega\nu_e$. The problem with the i-delta treatment is immediately obvious, because in a real system there is always a place where the fundamental mode is resonant, where $k_\parallel$ vanishes. This yields an electron conduction channel, of width $\Delta_D \equiv \sqrt{\omega_*\nu_e}/k_\parallel' V_e$, in which the fluctuations are hydrodynamic, *i. e.*, the flow fluctuations are decoupled from and not driven by those in the density, although the former can still drive the latter. Outside this region the fluctuations are adiabatic, as the plasma acts to short out the large parallel currents otherwise generated. The purpose of this paper is to demonstrate that for the single-helicity 2D case the nonadiabatic density response, $\widetilde{n}/n_0 - e\widetilde{\phi}/T$, and hence the cross-field particle fluxes are confined to the electron conduction channel, with the result that anomalous transport by drift waves over large regions in toroidal devices would have to be an inherently 3D process coupling many helicities.

II. The Model

The basic model for nonlinear drift-wave turbulence in this paper is a 2D sheared slab whose coordinate system of unit vectors $(\hat{\mathbf{x}}, \hat{\mathbf{y}}, \hat{\mathbf{z}})$ is defined respectively by the directions of the density gradient, the fundamental wavevector, $\mathbf{k}$, and the magnetic field at the resonant surface, where $k_\parallel = k'_\parallel x = 0$. The two-fluid Braginskii model[3] is used with the assumptions of electrostatic fluctuations ($\widetilde{\mathbf{B}} = 0$), a thin resonance layer ($k\Delta_D \ll 1$), and cold ions ($T_i \ll T_e \equiv T$). One then has the Ohm's law and equations for charge conservation, electron continuity, and parallel ion momentum, with the last included to provide for the linear damping mechanism of coupling to outward-propagating ion sound waves. If x, y, t and the normalised fluctuating variables are respectively scaled by $\rho_s, k^{-1}, \omega_*^{-1}$, and (ρ_s/L_n); we have the dimensionless system of equations used in this paper:

$$\frac{\partial}{\partial t}\nabla_\perp^2\phi = -\hat{\mathbf{z}}\cdot\nabla\phi\times\nabla(\nabla_\perp^2\phi) + C^{-1}\nabla_\parallel^2(n-\phi) + D(\nabla_\perp^2\phi), \tag{1}$$

$$\frac{\partial n}{\partial t} = -\hat{\mathbf{z}}\cdot\nabla\phi\times\nabla n - \frac{\partial\phi}{\partial y} + C^{-1}\nabla_\parallel^2(n-\phi) - S\nabla_\parallel u + D(n), \tag{2}$$

$$\frac{\partial u}{\partial t} = -\hat{\mathbf{z}}\cdot\nabla\phi\times\nabla u - S\nabla_\parallel n + \mu\nabla_\parallel^2 u + D(u). \tag{3}$$

In each, the first term is the nonlinear piece of the convective derivative, $\nabla_\parallel = x(\partial/\partial y)$, and D is a perpendicular operator used solely for numerical purposes to facilitate truncation of the spectrum in k_y-space. In order to study more clearly the character of the turbulence, we have not included artificial driving.

The parameters are the ratios $C \equiv (\Delta_D/\rho_s)^2 = (\nu_e/\omega_*)(m_e/M_i)(L_s/L_n)^2$ and $S \equiv L_n/L_s$, with the parallel diffusion coefficient $\mu \equiv \mu_\parallel/\rho_s^2\omega_*$, and the wavenumber scale $k\rho_s$. The most important is C, which determines the electron channel width. The diffusion coefficient in D is assumed to be sufficiently small that D has no effect at either the largest scales or those at ρ_s sizes. The scheme is finite-differenced in the x-direction and pseudospectral in y. A split timestep is used, evaluating the $\nabla_\parallel$ terms at mid-step and the D terms at the forward step. The fields are set to zero at some x_L, giving a spatial ordering of $(\Delta_D, \rho_s) < S^{-1} < \mu^{-1/2} < x_L < k^{-1}$. This places strict limits on all the parameters. One would like to vary C in particular over a wide range but this scheme has been limited to $.3 < C < 10$.

III. Resolution Considerations

The question of k-space resolution in numerical treatments of drift-wave turbulence is very important but often neglected. In particular, there are three scales in the problem which must be separated. These are the macroscopic gradient scale or experimental system size, the most probable structure size, typically on the order of a ρ_s, and the smallest scales at which the dissipation is acting to truncate the spectrum. The operator D serves to avoid pile-up of energy at the highest k's. However, a real plasma has such a high perpendicular Reynolds number that any important scales are practically inviscid. This is the reason the ρ_s scales must be kept out of the dissipation range of D. Most previous treatments have neglected this consideration,[4] leading to the erroneous conclusion that only the largest scales play important

roles in the physics. It is also important to separate the ρ_s scales from the largest to allow any structures which may form to interact on the largest scales.

IV. Results

Before going on to the results, a word on the identification of coherent structures in simulations of turbulence is in order. This is the fact that the eye cannot be depended on for this identification. A useful diagnostic in the identification of self-coherence is *kurtosis*, or flatness, defined for zero-mean fluctuations as $\mathrm{Ku}(\phi) \equiv \langle \phi^4 \rangle / \langle \phi^2 \rangle^2$, where the angle brackets represent ensemble averages, approximated in the simulation by all-space integrations. Suitably normalised, this has the value three for completely random fluctuations. A high value of Ku is the most reliable signature of self-coherence. This has been used before in studies of decaying Navier-Stokes turbulence,[5] but has been neglected in drift-wave simulations.

The computations are initialised with an isotropic, random-phase field multiplied by a spatial Gaussian envelope to reflect shear-localisation to the resonant surface, then normalised so that the rms velocity fluctuation is unity, *i. e.*, marginally nonlinear. Initially, the density is purely adiabatic, $h \equiv n - \phi = 0$. The parallel velocity is set to $u = Sx\phi$. This state is then evolved in time according to Eqs. (1-3).

There is not sufficient space to fully characterise the results, so the most important features are displayed in Figs. 1 and 2. In general terms, the fluctuations leave the initial state extremely quickly. As expected they are appreciable only within one to two Δ_D of the resonant surface. A moderately violent transient state is passed through in the first few tenths of an ω_*-time, after which the nonadiabatic response is strongly localised with a Δ_D and the kurtoses in all quantities have reached large values, 10-15 for the basic fields and well over 30 for the nonadiabatic response, h, which is also observed to decay much more slowly than either n or ϕ, increasingly dominating the total response.

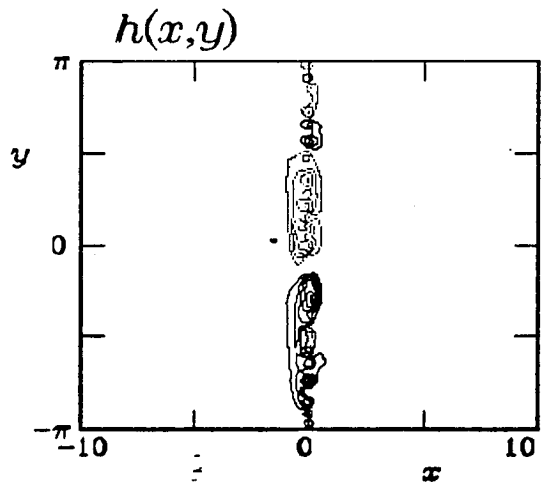

*Fig.*1. Solid contours have positive values; dotted, negative. The maximum is 0.844.

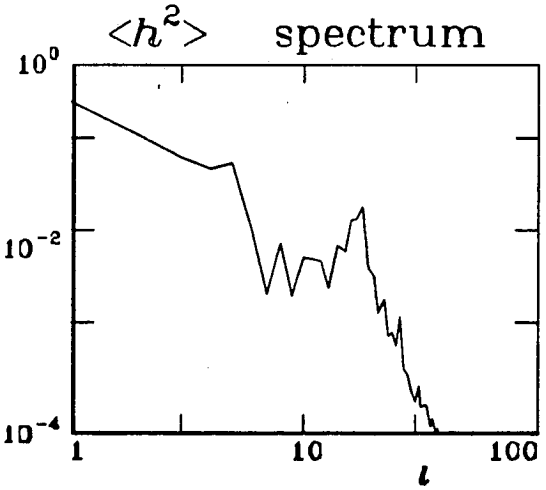

*Fig.*2. The brackets represent an integration over x. l is the mode number.

In Fig. 1 one sees the character of h, particularly the localisation within $x = C^{1/2}$ (1 for this case). The zero contour has been suppressed for clarity. Two dominant structures have formed of several smaller at intermediate scale. This behaviour is seen to persist throughout all the runs varying C. In each, the localisation closely tracks $C^{1/2}$, verifying Δ_D, not ρ_s, as the scale. The high kurtosis identifies the structure as self-coherent. More important than the absolute value is the fact that Ku(h) is a factor of 3 or so higher than Ku(ϕ) or Ku(n), *i. e.*, the character of h is so different from either n or ϕ that a simple phase relation between the latter is hoplessely inadequate. The spatial dependence of the actual relation is clear, as the fluctuations are adiabatic (as well as small) in the high-shear regions.

The complete dominance of the coherent structure in the nonadiabatic response is reflected in the k_y spectrum of h, shown in Fig. 2. Superimposed upon the intermediate range is a maximum at the $k_y \gtrsim \Delta_D^{-1}$ scale. The strength of the largest scale reflects the combination of the small structures into large ones. The steepness of the spectrum at high k indicates the dissipation range of D. As well, the steepness of the intermediate range (greater than the Komolgorov $E_k \sim k_y^{-3}$) reflects the effectiveness of *parallel* dissipation at all scales. It is questionable indeed whether a proper inertial range in the Komolgorov sense exists for the system Eqs. (1-3).

Observed selective decay between the energies in h and those in n and $\nabla\phi$ indicates the growing dominance of the nonadiabatic response in the hydrodynamic region. It is clear that an i-delta treatment can not explain the dominant features of 2D drift-wave turbulence. Lastly, tests of the simulation have verified that all of the foregoing is independent of the form or size of the operator D, so long as the perpendicular Reynolds numbers are large at the intermediate scales.

V. Transport

The major implication of this work at the present stage is that appreciable cross-field flux of density is possible only within one Δ_D of the resonant surface. Further away, the large shear forces the fluctuations to be both adiabatic and small. The tight localisation of the flux in this 2D simulation indicates that anomalous transport due to drift waves over large regions would have to be a 3D phenomenon, capable of supporting hydrodynamic behaviour everywhere. One other conclusion which must be qualified by the fact that an adequate 3D treatment has yet to be performed is that anomalous transport by drift-wave turbulence should be dominated by the dynamics of coherent structures.

References

[1]P. Liewer, *Nucl. Fusion* **25**, 543 (1985).

[2]A. Hasegawa and K. Mima, *Phys. Rev. Lett.* **39**, 205 (1977).

[3]S. I. Braginskii, in *Reviews of Plasma Physics*, edited by M. A. Leontovich (Consultants Bureau, N. Y., 1965), Vol. 1, p. 205.

[4]D. Biskamp, *Phys. Lett.* **109A**, 34 (1985); M. Wakatani and A. Hasegawa, *Phys. Fluids* **27**, 611 (1984); R. E. Waltz, *Phys. Fluids* **26**, 169 (1983).

[5]J. C. McWilliams, *J. Fluid Mech.* **146**, 21 (1984).

Fluctuations and Transport Measurements in the TEXT Tokamak[†]

Roger D. Bengtson, R.V. Bravenec, D.L. Brower,[‡] P.H. Diamond,
K.W. Gentle, C.C. Klepper, N.C. Luhmann, Jr., [‡] W. A. Peebles,[‡]
P.E. Phillips, E.J. Powers, T.L. Rhodes, B. Richards,
Ch.P. Ritz, W.L. Rowan, and A.J. Wootton

Physics Department and Fusion Research Center
The University of Texas at Austin
Austin, Texas 78712 *USA*

[‡]University of California at Los Angeles, Los Angeles, CA 90024.

Abstract

We present measurements of density and potential fluctuations under typical discharge conditions in the TEXT tokamak using Langmuir probe and far-infrared Thomson scattering techniques. A direct measurement of the fluctuation induced particle flux is presented and compared with global particle confinement measurements. Measurements of poloidal asymmetry and their effects on transport are discussed.

[†] Research is supported by DoE Contract DE-AC05-78ET53043 and Joint Services Electronics Program Contract F49620-82-C-0033.

Introduction

One of the primary limitations to improving particle and energy confinement in magnetic confinement devices is the small scale instabilities, which drive turbulence and may give rise to the observed anomalous transport. We present detailed experimental measurements of turbulence and transport and quantify the scalings with plasma parameters. The results can be compared with theoretical models.

Description of Apparatus

The measurements were performed on TEXT, an ohmically heated tokamak with major radius $R = 1.0m$ and limiter radius $a = 0.27m$. The limiter was a 360° circular titanium carbide ring whose front surface was 0.03 m from the stainless steel wall, at one toroidal position. Measurements have been made for discharges covering the parameter range of $I_p = 100 - 400kA, B_t = 1.0 - 2.8T, Z_{eff} \approx 2 - 4$, and a line averaged density $\bar{n}_e = 0.8 - 4 \times 10^{13} cm^{-3}$. Data were taken over a $50ms$ during the plateau region of sawtoothing discharges.

A four probe array, consisting of a square array of four single Langmuir probes with 2 mm separation between adjacent probes, was located at the top of the tokamak along the plasma centerline. Probes were either biased $160V$ into ion saturation to measure $n\sqrt{T}$ or unbiased to measure the plasma floating potential, φ. Temperature, T, is measured with a swept double probe. Space potential is computed from the floating potential and electron temperature. We assume temperature fluctuations to have a negligible contribution to our measurements. For most plasma conditions, the probes could be inserted $0.015m$ inside the limiter radius without perturbing the plasma.

Digital spectral analysis was used to reduce the information contained in the time series of $n(t)$ and $\varphi(t)$ obtained from the probe. The wavenumber k is measured from the phase delay between two probes. Estimation of $S(k, \omega)$ is based on a correlation technique proposed by Beall[1] et al. The radial particle flux Γ and its spectral distribution Γ_ω, due to electrostatic fluctuations, is computed from simultaneous measurements of the density ($\tilde{n}$) and potential ($\tilde{\varphi}$) fluctuations by ensemble averaging over many independent realizations

using

$$\Gamma = < \tilde{n}\tilde{v} > = 2 \sum_{\omega > 0} Re\{n_\omega v_\omega\} = 2 \sum_{\omega > 0} \Gamma_\omega$$

with

$$v_\omega = \frac{\tilde{E}_\theta \times B}{B^2} = ik_\omega \tilde{\varphi}_\omega / B$$

The six-channel far-infrared Thomson scattering system and calibration scheme employed for these measurements is described in Refs. 2 and 3. The entire $S(k,\omega)$ spectra is monitored during a single tokamak discharge with spatial resolution produced by translating the scattering system both horizontally and vertically to move the scattering volume within the plasma. The wave propagation direction was determined using single channel heterodyne and multichannel homodyne detection. The length of the scattering volume is dependent upon the scattering angle and varies from a chord average at $k = 0$ to $\pm 8cm$ at $k = 12cm^{-1}$.

Characterization of Turbulence

The complete $S(k,\omega)$ spectra for density fluctuations measured during a single tokamak discharge as is shown in Fig. 1. The dominant low wavenumber region ($k < 5$ cm $^{-1}$) is characterized for both scattering and probe data by a broad, but peaked spectrum with $\triangle\omega/\omega \approx \triangle k/k \approx 0.5$. The contour plot obtained from the probe data also indicates that the fluctuating power above $k_\theta = 7$ cm^{-1} is small. The $S(k_\theta)$ exhibits a broad peak at $k_\theta \approx 2 - 4\text{cm}^{-1}(k_\theta \rho_s = 0.1)$ with a fall off proportional to $k_\theta^{-4 \pm 0.5}$ for larger wave numbers.

The two-dimensional structure of the turbulence was studied using an array of four probes separated both radially and poloidally by a small separation $\triangle x \approx 2mm$. The probe tips are not the innermost points of the probe body, so that the perturbation to the plasma may be enhanced. The method used to estimate $S(k_r, k_\theta, \omega)$ is similar to the statistical dispersion relation approach[1] for a single k component. In Figure 2 the frequency integrated spectrum $S(k_r, k_\theta \omega)$ is shown for a radial location $r = 255mm$. The $S(k_r, k_\theta)$ spectrum is broader in the radial direction than in the poloidal direction. This anisotropy is quantified by the half width $\sigma(k)$ of the spectrum: we typically find $\sigma(k_r)/\sigma(k_\theta) \approx 2$.

From the $S(k_\theta,\omega)$ spectrum we compute the power weighted phase velocity using $v_{ph}(\omega) = \sum_{\omega,k}(\omega/k)S(k,\omega)/\sum_{\omega,k} S(k,\omega)$. The phase velocity is nearly independent of frequency for $f \leq 100kHz$. Figure 3 presents the measured phase velocity for both density and potential fluctuations as a function of radius. Note that the phase velocity changes from propagation in the electron diamagnetic direction in the bulk plasma to propagation in the ion diamagnetic direction behind the limiter. This can be explained by a radial electric field that produces a $E_r \times B$ rotation. Also shown in Figure 3 is the profile of the plasma potential from which the radial electric field is derived. The dominant contribution to the measured plasma rotation at the outer edge is from the measured E_r. The remaining contribution is from the pressure gradient drift velocity and is consistent with measured density and temperature profiles. Scattering data from the same interaction region as the probes gave the same velocity. As the scattering volume was moved towards the plasma center, the measured phase velocity remained constant.

In the region of highest velocity shear (dv/dr) we observe additional broadening of the spectra. This cannot be explained by an $E_r \times B$ Doppler shift of the rotating plasma, which will cause a change in measured phase velocity but not a change in spectral width. The high shear region extends over approximately $10mm$ and is located $\sim 10mm$ inside the limiter radius. In this region the turbulence becomes isotropic $(\sigma(k_r)/\sigma(k_\theta) \approx 1)$ in contrast to the low velocity shear regions. The correlation of a vorticity maximum with spectral isotropy and broadened spectra may be indicative of shear flow drive turbulence.

Density and potential fluctuations peak $5 - 10mm$ inside the main plasma. The scattered power peaks at the limiter with a spatial width larger than the estimated spatial resolution. For normal operation, the fluctuation level is significantly larger at the top of the plasma than at the bottom demonstrating a poloidal asymmetry in turbulence. This asymmetry[6] inverted with a reversal of the plasma current. Measurements with probes located at multiple poloidal positions and one toroidal location show an up-down asymmetry in the fluctuation amplitudes but not in density and temperature profiles. At the outer equator of the plasma, the density, temperature, potential and fluctuation profiles are different from those at the top and bottom. These asymmetries are not understood and work is continuing.

The radial profiles of the frequency integrated density and potential fluctuations are significantly different. A consequence of this is that the Boltzmann relation does not hold in the edge plasma. This is shown clearly in Figure 4 where $e\tilde{\varphi}/kT$ is larger than $\tilde{n}/n$ for probe locations inside the limiter. The fact that the Boltzmann relationship is not satisfied throughout the edge region means that an estimate of particle flux requires a simultaneous measurement of density and potential fluctuations and the phase angle between them.

Transport

An estimate of the fluctuation induced particle flux due to $\tilde{E}_\theta \times B$ drift as is shown in Figure 5. The flux peaks at the radial location where $\tilde{n}$ and $\tilde{\varphi}$ are maximum, approximately $10mm$ inside the limiter radius. The phase angle of the density fluctuations relative to the potential fluctuations is close to 90° for the dominant fluctuation power at frequencies below $200kHz$. The sign of the average poloidal wavenumber $\bar{k}(\omega)$ changes going through the high velocity shear region but the particle flux is always outward because the phase angle also changes sign. To maintain continuity, an additional convection mechanism must be invoked. Possible mechanisms to maintain continuity are a radial flow or poloidal/toroidal convection of particles due to asymmetries.

Comparisons with predictions of density gradient driven[7] (∇n) and resistivity gradient driven[8] ($\nabla \eta$) models have been carried out. The resistivity gradient driven model scales better with radius because of its favorable temperature dependence. More data is needed to compare models with experimental results.

From the fluctuation induced particle flux measurement at one poloidal and toroidal location, we can, with the assumption of symmetry, estimate the particle confinement time by $\tau_p(a) = N/(\Gamma(a)A)$ where N is the total number of particles in the plasma and A is the area of the outer surface defined by limiter contact. Typical results for τ_p as a function of electron density are shown in Figure 6 and compared with measurements of the global particle confinement time deduced from measurements of the source function using H_α. The scaling of fluctuation induced particle flux with the global measurements of confinement time is in agreement and the absolute values of τ_p are well within possible errors. This agreement may be coincidental as the probe measurements do not take into account

the known poloidal asymmetries in the plasma, but the scalings with I_p, B_T, *and* $\bar{n}_e$ are identical with the errors, suggesting a causal relationship.

We have attempted to estimate the electron heat flux due to fluctuations where $q_{conv} = 5/2kT_e\Gamma$, $q_{cond} = 5/2kn_e < \tilde{T}\tilde{E} > /B$. Magnetic fluctuation induced flux was also considered. The electron heat fluxes are shown in Figure 7 where $q_{tot} = q_{cond} + q_{conv}$. Note that the convective contribution to the total heat flux is small. Electrostatic fluctuations cannot explain the conducted heat flux for this low density discharge: a value of $\tilde{T}/T > 1$ would be required. The contribution of the magnetic fluctuations to the heat conduction in the edge appears to be negligible because of the small levels measured ($\tilde{B}_r/B_T \approx 10^{-4}$). The contribution of electrostatic fluctuations to the total heat flux may become more important at higher densities. We have seen from both source and fluctuation measurements that q_{conv} is approximately independent of density as the temperature drop with increasing $\bar{n}_e$ at the limiter compensates for the increasing particle flux with increasing density. More results and theory are required to verify these results.

Acknowledgements

The authors wish to thank the TEXT staff for their assistance.

References

1. J.M. Beall, Y.C. Kim, E.J. Powers, J. Appl. Phys. **53**, 3933 (1982).
2. H. Park, C.X. Yu, W.A. Peebles, N.C. Luhmann, Jr., R. Savage, Rev. Sci. Instrum. **53**, 1535 (1982).
3. H. Park, D.L. Brower, W.A. Peebles, N.C. Luhmann, Jr., R.L. Savage, Jr., C.X. Yu, Rev. Sci. Instrum. **56**, 1055 (1985).
4. Ch.P. Ritz, R.D. Bengtson, S.J. Levinson, E.J. Powers, Phys. Fluids **27**, 2956 (1984).
5. S.J. Levinson, J.M. Beall, E.J. Powers, R.D. Bengtson, Nucl. Fusion **24**, 527 (1984).
6. D.L. Brower, W.A. Peebles, N.C. Luhmann, Jr., R.L. Savage, Jr., Phys. Rev. Lett. **54**, 689 (1985).
7. P.W. Terry and P.H. Diamond, Phys. Fluids **28**, 1419 (1985).
8. L. Garcia, P.H. Diamond, B.A.Carreras, and J.D. Callen, Phys. Fluids **28**, 2147 (1985).

Figure Captions

1. $S(k_\theta, \omega)$ spectra at $r = 25.5cm$ for Langmuir probes (contours) and FIR scattering (bars indicate spectral linewidth).
2. Frequency integrated spectrum $S(k_r, k_\theta)$ from Langmuir probes, measured at the top of the tokamak at $r = 25.5\ cm$.
3. Radial profiles of the plasma potential and of the poloidal phase velocity in the lab frame measured with Langmuir probes.
4. Radial profiles of potential $e\tilde{\varphi}/kT$ and $\tilde{n}/n$ density fluctuations from Langmuir probes. Also shown is the edge value $\tilde{n}/n$ from scattering data.
5. Radial profile of the radial particle flux induced by electrostatic fluctuations.
6. Global particle confinement (+) and particle confinement predicted from electrostatic fluctuation measurements (0) versus chord-averaged electron density. For this scan $B_T = 2.0T, I_p = 200kA$.
7. Electron radial heat fluxes due to convection obtained from source measurement and conduction obtained from power obtained from power balance analysis.

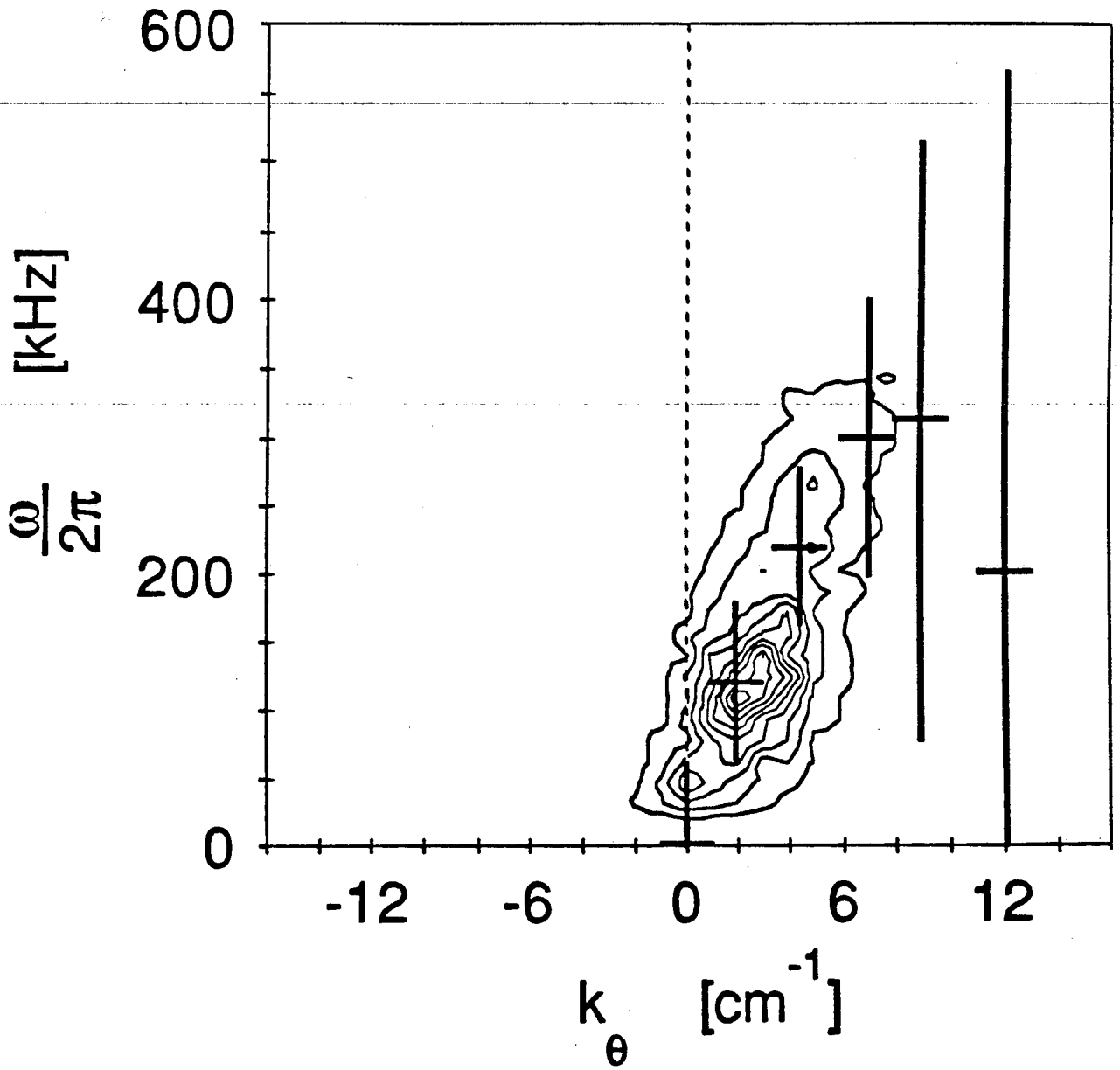

Figure 1.

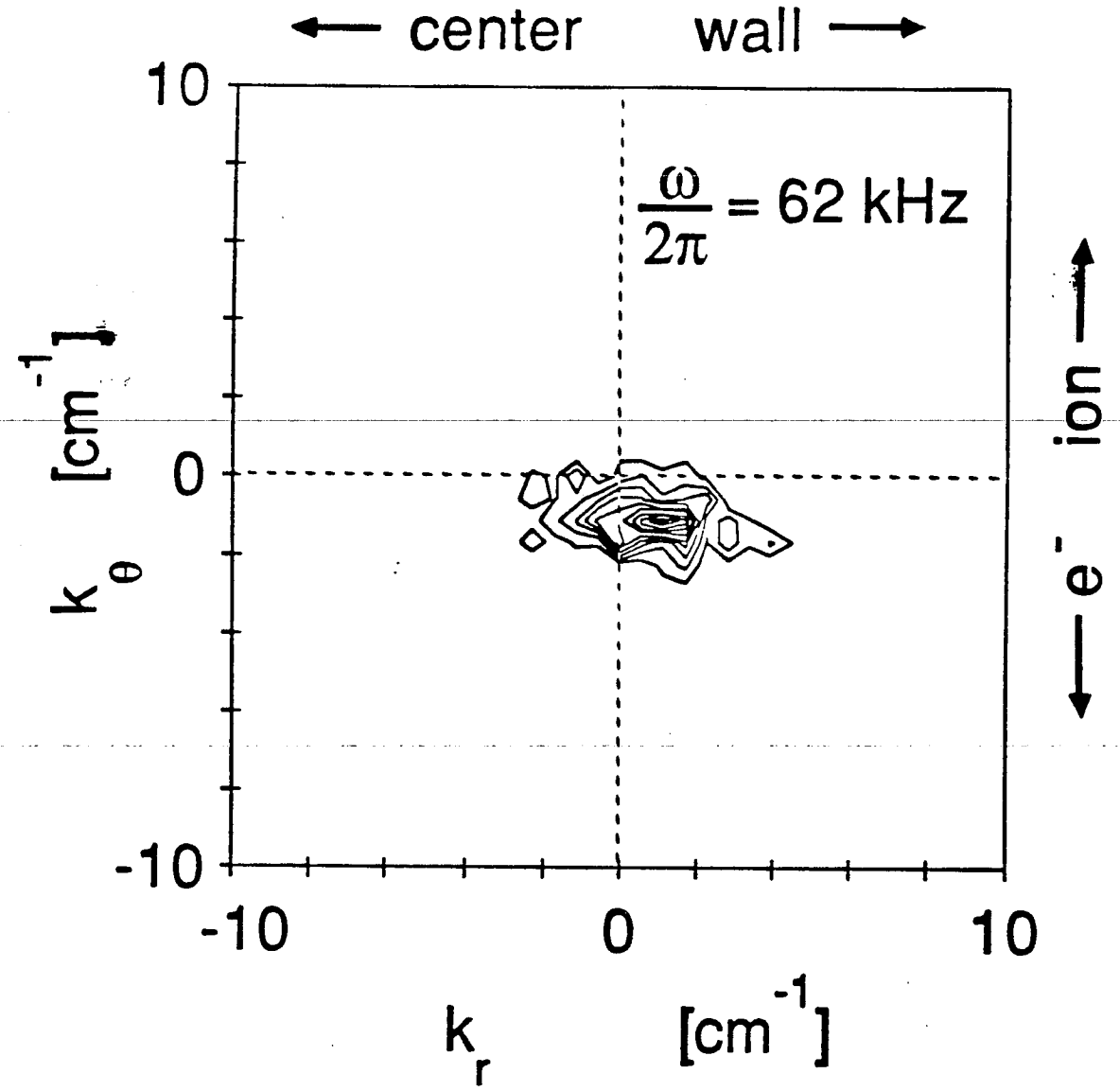
center
wall
10
0
-10
-10
0
10
$\frac{\omega}{2\pi}$ = 62 kHz
k_θ [cm^{-1}]
k_r [cm^{-1}]
ion
e$^-$

Figure 2.

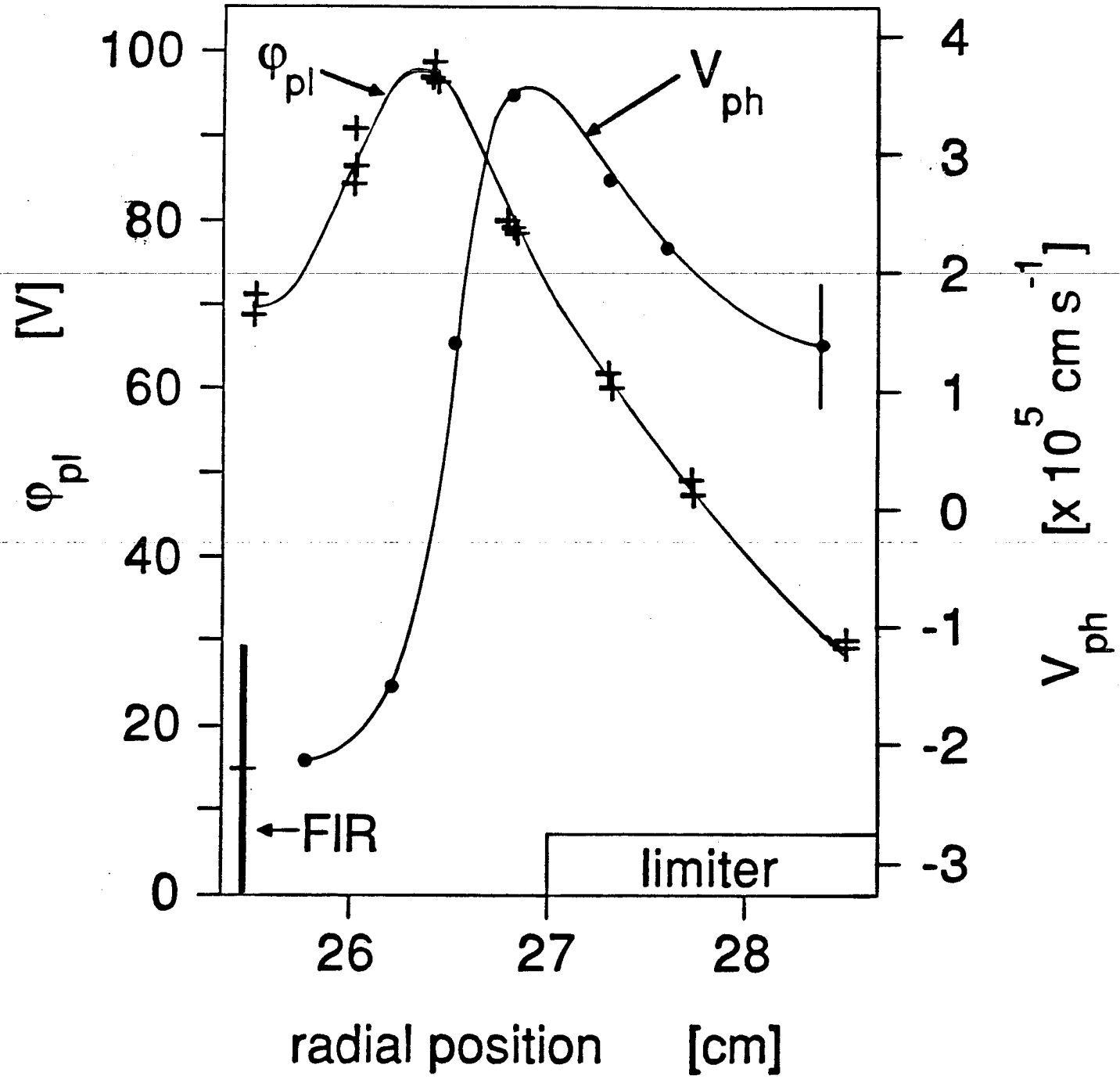
100
80
60
40
20
0
φpl [V]
4
3
2
1
0
-1
-2
-3
Vph [x 10^5 cm s^-1]
φpl
Vph
FIR
limiter
26
27
28
radial position [cm]

Figure 3.

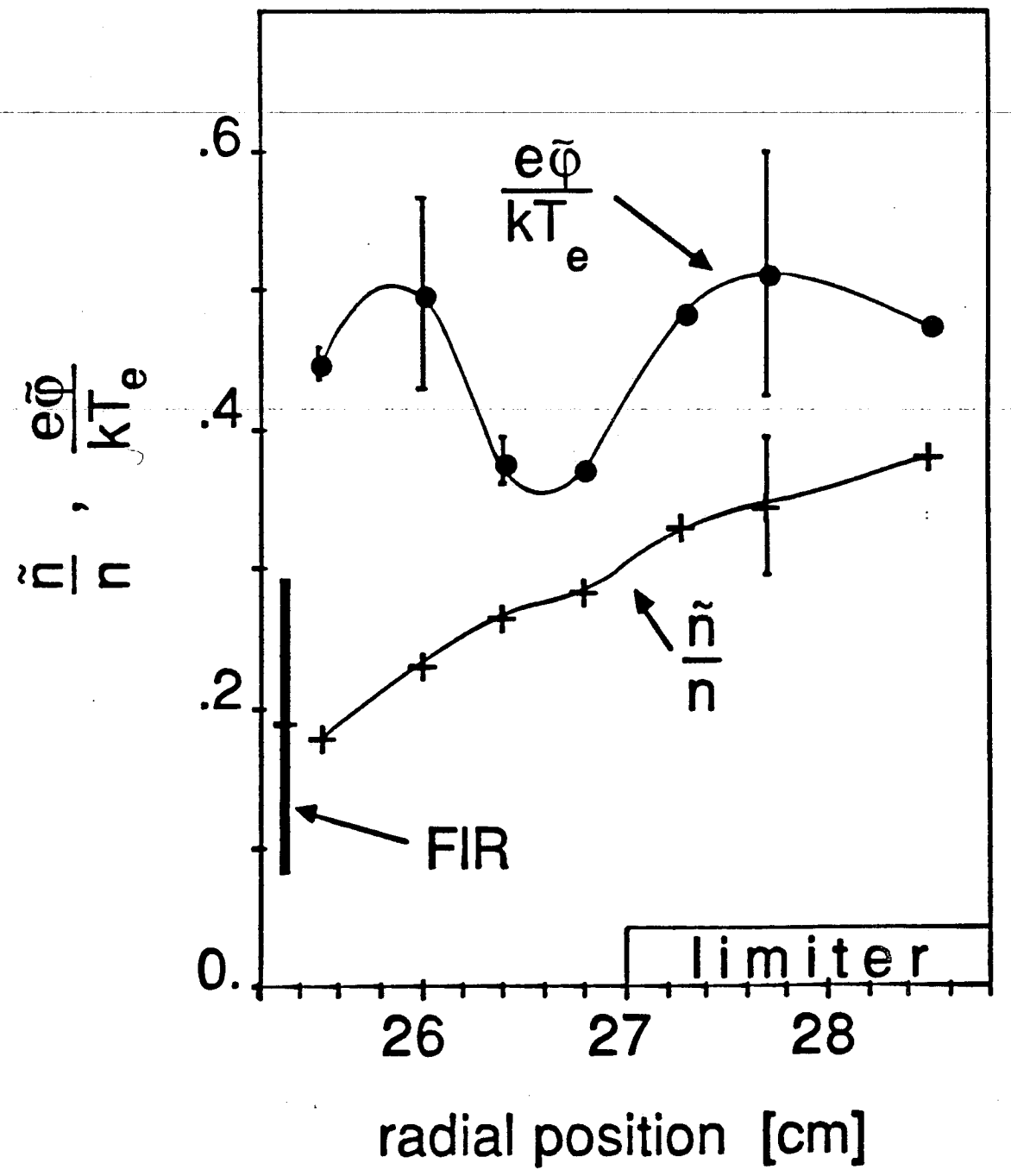
.6
.4
.2
0.
$\frac{e\tilde{\varphi}}{kT_e}$
$\frac{\tilde{n}}{n}$, $\frac{e\tilde{\varphi}}{kT_e}$
$\frac{\tilde{n}}{n}$
FIR
limiter
26
27
28
radial position [cm]

Figure 4.

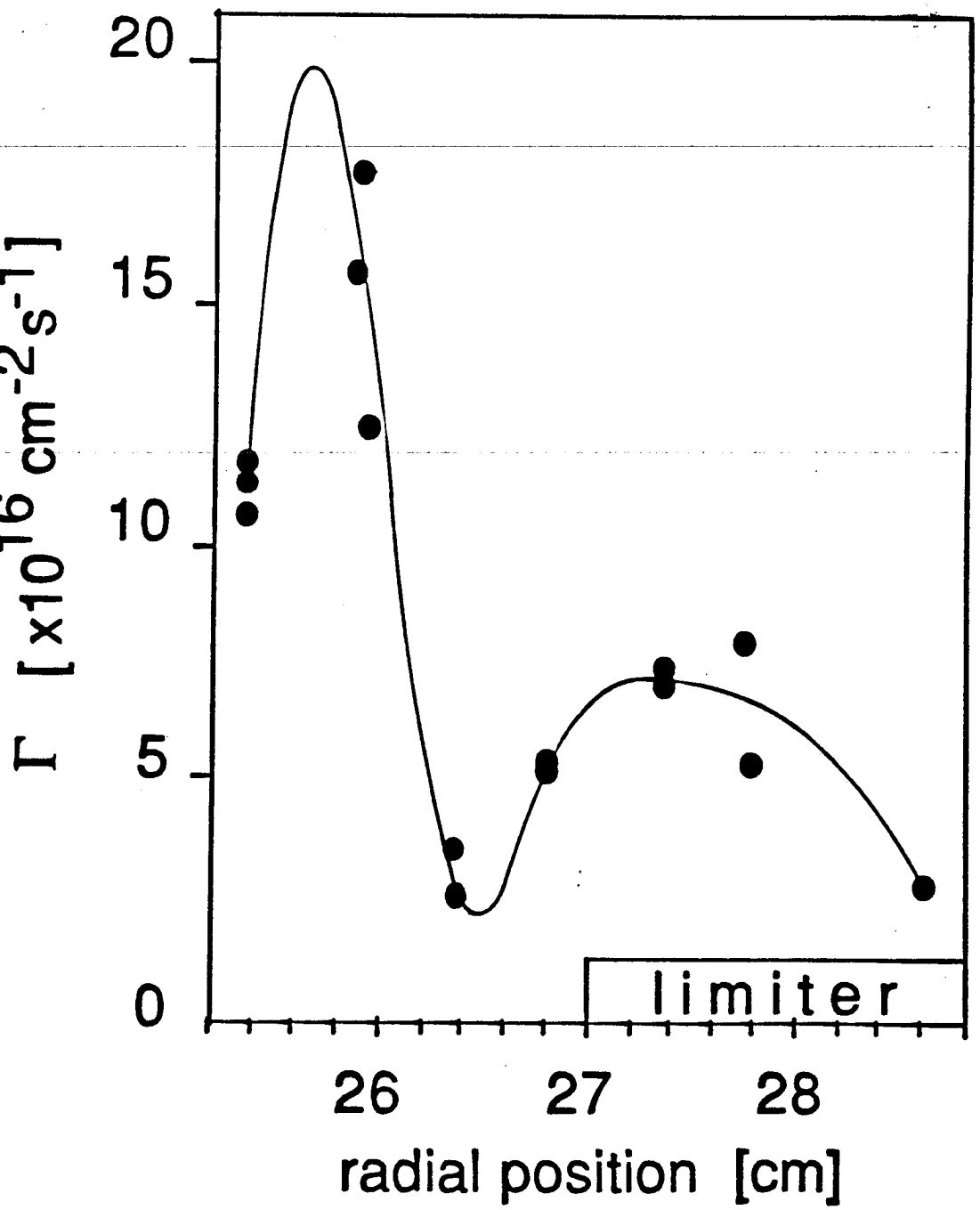

Figure 5.

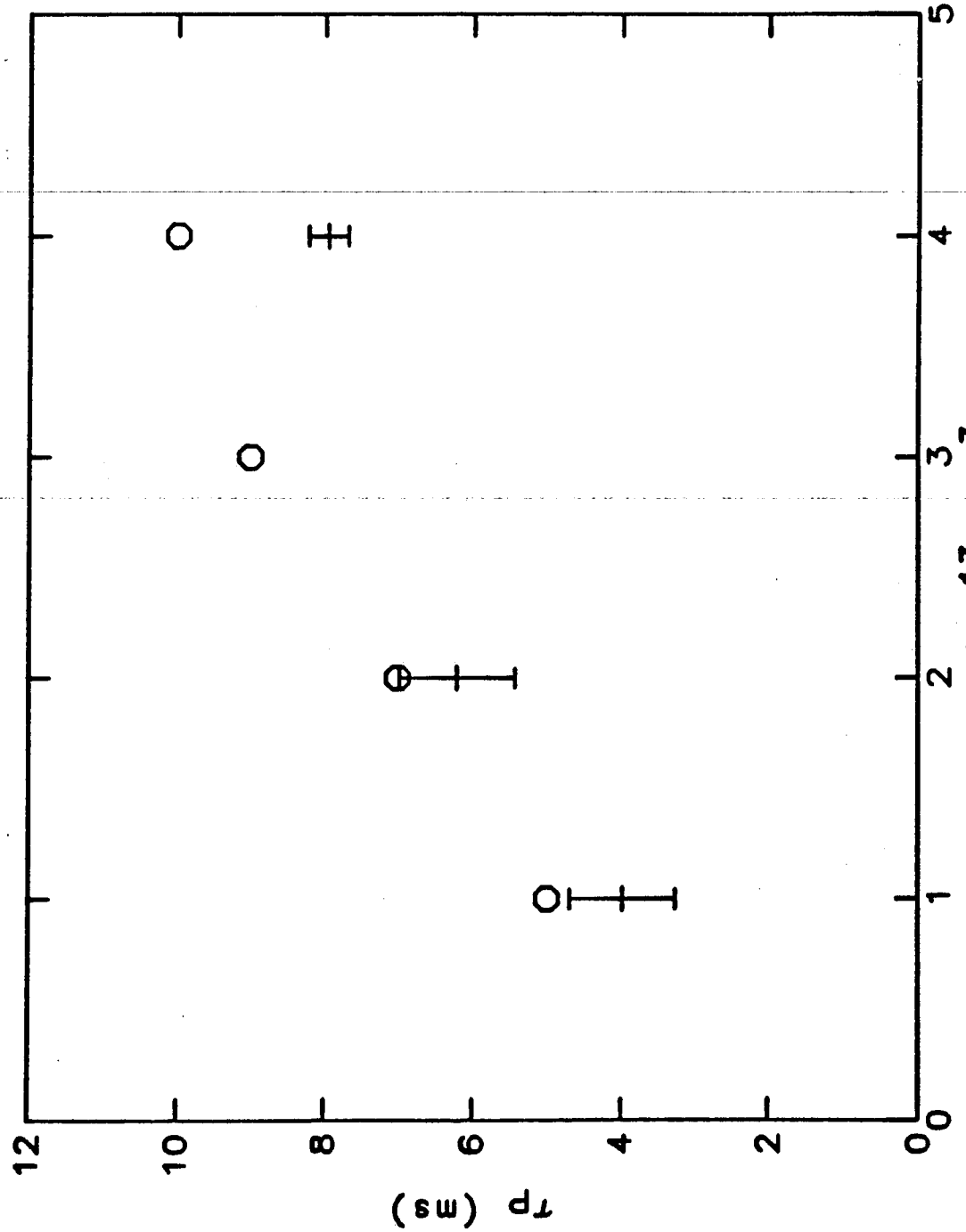

Figure 6.

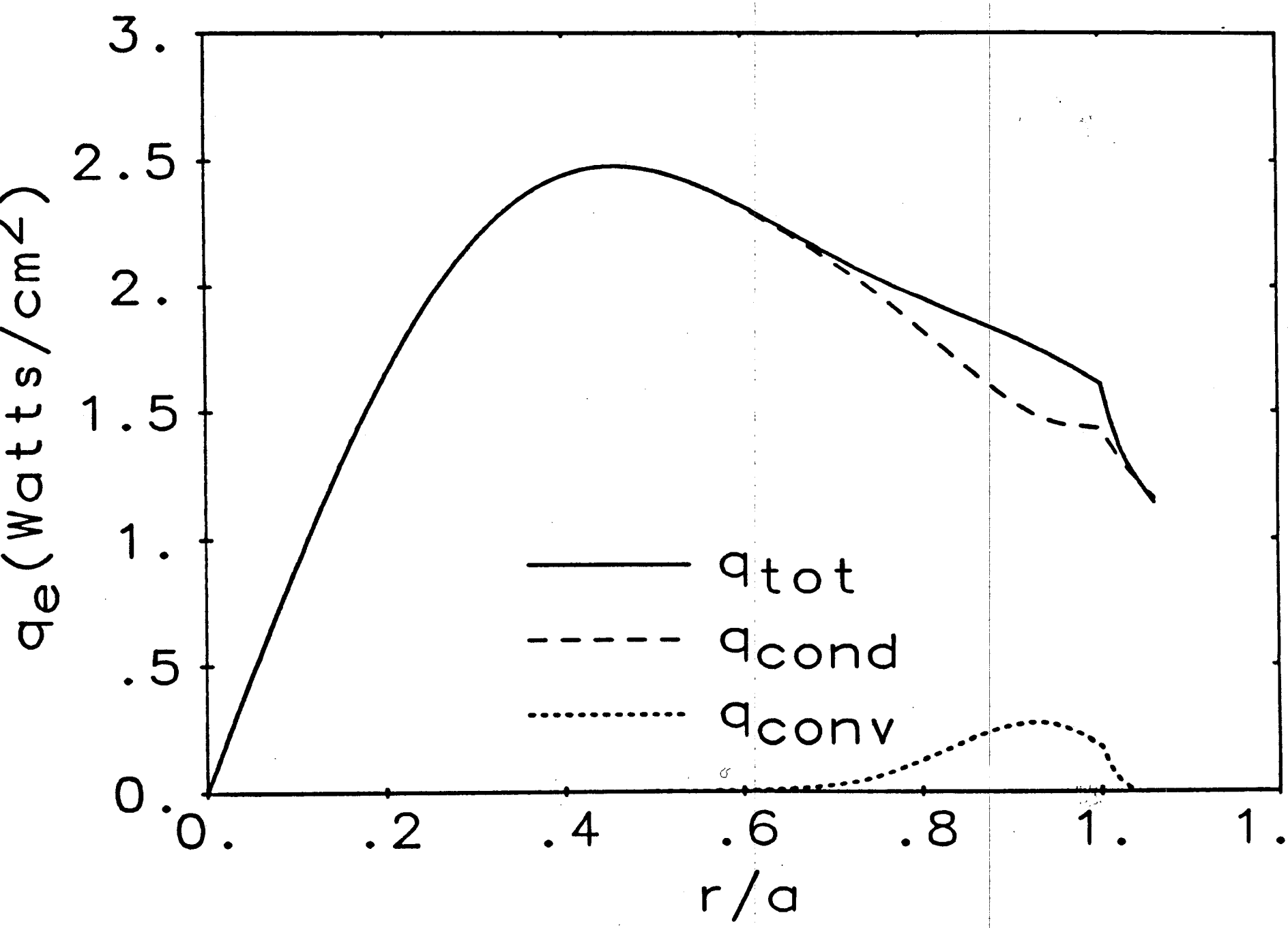

Figure 7.

Ion Pressure Gradient Driven Turbulence: Theory and Consequences

P. H. Diamond, G. S. Lee, N. Mattor,* and *P. T. Katt*†

Institute for Fusion Studies

The University of Texas at Austin

Austin, Texas 78712-1060

Abstract

Ion pressure gradient driven turbulence (IPGDT) due to η_i-modes is of interest both as a paradigm for saturated, multifield turbulence and as an agent for anomalous transport in fusion devices. The results of recent investigations of IPGDT are summarized. Special emphases are placed on the validity of "mixing length rules" and on the relation of ion thermal transport to particle confinement. The possible role of IPGDT in RFP plasmas is discussed.

* Present Address: Oak Ridge National Lab

† Also Department of Physics

Introduction

In this paper the results of recent investigations[1] of ion pressure gradient turbulence are summarized. Ion pressure gradient driven turbulence (IPGDT) is of interest both as a paradigm for saturated multifield turbulence and as an agent for anomalous transport in tokamaks. Here, the theory and consequences of IPGDT are discussed. Special emphases are placed on the validity of "mixing length rules" and on the relation of ion thermal transport to particle confinement. The possible roles of IPGDT in RFP and stellarator plasmas are also discussed. This paper is divided into two sections. Part I is concerned with the basic theory IPGDT, while Part II discusses applications to anomalous transport in fusion devices.

Part I: IPGDT—Theory

IPGDT develops from unstable η_i-modes[2] which are incompressible mass-flows resulting from the coupling of sound waves to radial ion temperature gradients. For $\eta_i > \eta_{i\,\mathrm{crit}} \sim 1.5$, IPGDT can be described by coupled fluid equations for vorticity $\left(\nabla_\perp^2 \phi\right)$, parallel flow velocity $(v_\parallel)$, and ion pressure $(\hat{p})$. Typical time and space scales characteristic of long wavelength η_i-modes are $\gamma \sim \left[(1+\eta_i)/\tau\right]^{1/2} k_\theta \rho_s c_s / L_s$ and $\Delta x \sim \left[(1+\eta_i)/\tau\right]^{1/2} \rho_s$. Shorter wavelength modes develop $\omega_r \sim \gamma$ as $k_\theta \rho_s \to 1$. Ultimately, ion Landau damping, represented in the fluid model as a parallel ion viscosity, truncates the spectrum at $k_\theta \rho_s \sim 1$.

A natural description for the nonlinear fluctuation dynamics of IPGDT utilizes coupled equations for the "energies" $E_w \sim \left\langle \hat{\phi}^2 + (\nabla \hat{\phi})^2 \right\rangle$, $E_k \sim \left\langle \hat{v}_\parallel^2 \right\rangle$, $E_p \sim \left\langle \hat{p}^2 \right\rangle$, thus ensuring consistency with the conservation laws and constraints of the system. The energy evolution is determined by physical processes characterized by three time scales, which are $\tau_{c,k} \simeq \left(D_k / \Delta x_k^2\right)^{-1}$, the nonlinear interaction time; $\tau_{\mathrm{eq},k} \simeq \left[\left((1+\eta_i)/\tau\right)^{1/2} \gamma_k\right]^{-1}$, the sound wave energy equipartition time; and $\tau_{d,k} = \left[\mu_\parallel k_\theta^2 \Delta x_k^2 / L_s^2\right]^{-1}$, the dissipation time scale. For IPGDT, the time scales follow the hierarchy $\tau_{\mathrm{eq},k} < \tau_{c,k} < \tau_{d,k}$. Hence, exploiting the fact that all nonlinearities are convective, the energy equations may be added so that the total energy ε is determined by

$$\frac{\partial \varepsilon}{\partial t} - \mu_\parallel \nabla_\parallel^2 \varepsilon + T_{1,2} \varepsilon = S_{1,2}^{(0)}. \tag{1}$$

Here, $T_{1,2}$ and $S_{1,2}^{(0)}$ refer schematically to the triplet and gradient source, respectively.

Standard methods of renormalization and stochastic models can now be employed to solve Eq. (1). A "Reynolds number" $\mathrm{Re} = T_{1,2}/\mu\nabla_{\|}^2 \sim \left[L_s^2 D_k/\mu_{\|} k^2 \Delta_k^4\right] \simeq (1+\eta_i)$ can be defined. As $\mathrm{Re} \gg 1$, coupling to smaller scales broadens the spectrum to $k_d \sim (\mathrm{Re})^{1/2} k_0$, where $k_0 \rho_s \sim 0.4$. Thus, corrections to "mixing length rule" estimates are significant! In particular, the predicted ion thermal diffusivity $\chi_i \sim \chi_{\mathrm{ml}} |C(\mathrm{Re})|^2$, where $\chi_{\mathrm{ml}} \sim \gamma(\Delta x)^2$, and $C(\mathrm{Re}) \simeq \pi/2 \ln(\mathrm{Re})$.

It is interesting to note that mixing length[3] and scaling methods,[4] which effectively balance $T_{1,2}\varepsilon \sim S_{1,2}$, ignore dissipation scales and are hence frequently applied to equations which do not even have a stationary solution! Indeed, note that $C(\mathrm{Re}) \to \infty$ as $\mu_{\|} \to 0$. Alternatively, even if "inertial" range properties are insensitive to $\mu_{\|}$, macroscopic observables are determined by spectrum sums, whose limits of integration depend on dissipation.

Part II: IPGDT—Consequences

Several transport coefficients of practical interest have been computed. These are:

i) the ion thermal diffusivity χ_i,

$$\chi_i = 0.4 \left(\frac{\pi^2}{4} \ln^2(1+\eta_i)\right) (\rho_s^2 c_s/L_s) \left(\frac{(1+\eta_i)}{\tau}\right)^2, \tag{2}$$

ii) the accompanying electron thermal diffusivity χ_e,

$$\chi_e = \varepsilon^{3/2} \left(\frac{\pi^2}{4} \ln^2(1+\eta_i)\right)^2 \left(\frac{1+\eta_i}{\tau}\right)^3 \frac{c_s^2 \rho_s^2}{\gamma_e L_s^2}, \tag{3}$$

iii) the particle diffusivity for $\gamma_* < 1$, and the particle flux for $\gamma_{ei} > \omega_{Te}$,

$$D_n \simeq \varepsilon^{3/2} \left(\frac{\pi^2}{4} \ln^2(1+\eta_i)\right)^2 \left(\frac{1+\eta_i}{\tau}\right)^3 \frac{c_s^2 \rho_s^2}{\gamma_e L_s^2} (2 + 3/2\eta_e), \tag{4a}$$

$$\langle V_r \rangle \simeq \left(\frac{\pi^2}{4} \left(\ln^2(1+\eta_i)\right)\right)^2 \left(1 - \frac{\eta_e}{\eta_e^c}\right) (0.5) \frac{\gamma_e}{L_n} \left(\frac{1+\eta_i}{\tau}\right)^2 \rho_s^2 \frac{m_e}{m_i}, \tag{4b}$$

iv) the ion (toroidal-flow) viscosity

$$\mu_{\perp} \simeq \chi_i \tag{5}$$

It is interesting to note that $\chi_i \sim (1+\eta_i)^2$, so that $\eta_i \gg \eta_{i\,\mathrm{crit}}$ is unlikely. Also, while Eq. (4b) predicts an inward pinch[5] for $\eta_e > \eta_e^c$, Eq. (4a) indicates that IPGDT-induced fluxes are *outward only*, for $\gamma_* < 1$. Thus, D_n drops with χ_i, consistent with the results of experiments,[6] where particle confinement improves after pellet injection. Similarly, Eq. (3) indicates that χ_e should also decrease with η_i, although other loss mechanisms may be operative. Finally, Eq. (5) follows from the fact that η_i-modes are sound waves, and thus naturally couple to ion flows.

IPGDT fluctuations are difficult to distinguish from the more familiar drift wave type, except in regards to direction of propagation (ion, rather than electron, diamagnetic). More generally, a possible clue would be the presence of fluctuations in flat density regions of ohmic saturation plasmas, where drift-wave turbulence should be weak.

It is interesting to note that an impurity species with charge Z, density n_{o_I} and scale length L_{n_I} modifies IPGDT according to the substitution rule $(1+\eta_i) \rightarrow (1+\eta_i)\left[1+Z\left(n_{o_I}/n_0\right)\left(L_n/L_{nI}\right)\right]^{-1}$. Thus, edge-peaked impurity concentrations enhance the turbulence while centrally peaked concentrations quench it. In particular, for Z-mode[7] plasmas in ISX-B, impurity injection was observed to improve particle confinement and steepen the density profile during auxiliary heating. This result is consistent with the predicted impurity enhancement of the IPGDT-driven inward flow.

Most of this discussion has focused on applications to pellet injection and neutral beam heating in tokamaks. However, η_i-modes are also possible in RFP and stellarator devices. In particular, in RFP plasmas, η_i-modes and resistive interchange modes couple naturally.[8] Thus, the non-adiabatic electron $\left(k_\parallel^2 v_{Th}^2 < \omega\gamma\right)$ resistive interchange smoothly connects to the adiabatic electron $\left(k_\parallel^2 v_{Th}^2 > \omega\gamma\right)$ η_i-mode of higher temperatures. It follows that η_i-mode turbulence is very likely in high temperature RFP plasmas, where density profiles are rather flat and strong ion heating occurs. Balancing η_i-mode induced thermal loss with ohmic heating yields the scaling $T \sim I_p^{3/4}\left(I_p/N\right)^{1/4}$. Hence, pellet injection should be considered in order to improve RFP energy confinement. Indeed, pellet injection may be a necessity for ignition at reasonable currents.

Stimulating discussions with M. Greenwald, F. Wagner, S. Wolfe, and A. J. Wootton

are acknowledged. This work was supported by the U. S. Department of Energy Contract #DE-FG05-80ET-53088.

References

1. G. S. Lee and P. H. Diamond, IFSR #209 (1986), accepted for publication in Phys. Fluids; N. Mattor, P. H. Diamond, and G. S. Lee, Sherwood Theory Meeting, 1986.
2. B. Coppi, et al., Phys. Fluids **10**, 582 (1967).
3. Conventional wisdom.
4. J. W. Connor, Nucl. Fusion **26**, 193 (1986).
5. B. Coppi and C. Spight, Phys. Rev. Lett. **41**, 551 (1978).
6. M. Greenwald, et al., *IAEA 1984*, Vol. 1, pp. 45.
7. Reference 1.
8. Z. G. An, et al., *Proc. of Compact Toroid Theory Workshop* (1984).

Localized Fluctuations in Inhomogeneous Plasma Turbulence; Structure, Dynamics, Relaxation, and Transport

P.W. Terry, P.H. Diamond, and T.S. Hahm

Institute for Fusion Studies
The University of Texas at Austin
Austin, Texas 78712-1060

Abstract

Localized fluctuations which are either decaying of self-binding are an important component of plasma turbulence often neglected in conventional treatments. Both types of localized fluctuations are described in the context of 3-D drift kinetic systems. Their role in plasma stability and transport is emphasized.

Introduction

Conventional descriptions of plasma microturbulence rely on a simple picture in which turbulence consists of a homogeneous ensemble of randomly phased, finite amplitude waves. Relative turbulent scattering of neighboring phase space trajectories is spacially uniform in such descriptions, implying that any tendency of the plasma to form localized, temporally decaying structures is not accounted for. Futhermore, the assumptions of statistical homogeneity and the random phase approximation which are employed in order to obtain a closure, do not allow for localized coherent structures in which self-field effects produce very long lifetimes relative to typical correlation times. Recent experimental results indicate that plasma turbulence may be more accurately viewed as an intermittent, spotty pattern of localized, nonlinear structures[1]. In this paper, several such structures intrinsic to low frequency turbulence in magnetized plasmas are described. More importantly, the role of these strongly nonlinear structures in anomalous transport and stability is emphasized. Of Particular note is the novel result that collisionless drift Alfven turbulence does not drive magnetic-flutter transport.

For some time it has been recognized that closely separated phase space trajectories turbulently scatter apart from each other at a rate which is slower than that of more distant trajectories[2]. Phase space density, which is conserved along such trajectories, thus tends to exhibit short range correlation. This correlation eventually decays under the turbulent scattering, but its lifetime may exceed the correlation time of the turbulence, which is determined by the longer scales associated with wave-like fluctuations. When the average distribution possesses a gradient, turbulent rearrangement of the average distribution actually creates phase space correlation. A balance between this source of correlation and the decay by inhomogeneous relative turbulent diffusion gives rise to a steady state in which the two-point phase space density correlation is highly peaked at small separation. This statistical correlation of phase space density at short range is referred to by the name of clumps. Because clumps are driven by the turbulent

rearrangement of average density, they represent a source of nonlinear plasma instability. Through the mechanism of phase space density conservation, this instability naturally relates to relaxation of the average distribution and transport. Nonlinear stability and transport in steady state turbulence for low frequency drift kinetic systems is detailed in Ref. 3.

In the two-point formulation used to describe clump phenomena, there is no simple way to incorporate the effects of the self-electric field associated with a localized clump of charged particles. Yet, simple estimates show that such fields can be sufficient to trap the particles that produced them[4]. Progress has been made in examining these self-trapping effects by studying single, isolated self-binding structures. Originally investigated in a 1-D geometry[4], we consider here phase space holes in the 3-D geometry of a drift kinetic system.

Electrostatic Drift Holes

A phase space hole is a depression in the phase space density distribution. Particles localized in the phase space region occupied by the hole are trapped by the potential well which they and the background plasma, consisting of passing particles, self-consistently produce. By definition, the drift hole is a steady state solution of the drift kinetic equation which satisfies a constraint of maximum entropy subject to a given mass, momentum and energy. The coherent structure studied here thus represents a most probable configuration of the system. We consider a simple hole in which the trapped particle density is taken to be constant in a rectangular region in phase space bounded by $|x| < \Delta x/2$, $|y| < \Delta y/2$, $|v_{\parallel} - u_{\parallel}| < \Delta v_{\parallel}/2$, where $u_{\parallel}$ is the center of mass hole velocity along the magnetic field line. The characteristic hole scales Δx, Δy, and $\Delta v_{\parallel}$ are obtained by maximizing the entropy $\sigma = -n_o \Delta x \Delta y \Delta v_{\parallel} [\tilde{f}(1 + \ell n f_o) + 1/2\ \tilde{f}/f_o^2]$ subject to fixed mass, $M = m_e \tilde{f} \Delta x \Delta y \Delta v_{\parallel}$, momentum, $P = M u_{\parallel}$, and energy $E = (M/24)\Delta v_{\parallel}^2 - |e|/2 \int dV \tilde{f} \phi(x)$ where n_o is the density, $\tilde{f}$ is the trapped particle phase space density, f_o is the background phase space plasma density, $\phi(x)$ is the self potential, and the energy integral is over the phase space volume of the trapped particles. The potential satisfies the quasineutrality condition

$$\left(1 - \rho_s^2 \left(\frac{\partial^2}{\partial x^2} + \frac{\partial^2}{\partial y^2}\right) + \frac{i v_{de} \partial/\partial y}{\omega}\right) \frac{|e|\phi(x)}{T_e} = \frac{-\tilde{f} \Delta v_{\parallel}}{n_o} \qquad (1)$$

where the left hand side represents the dynamics of passing particles: adiabatic electrons and ions with polarization and diamagnetic ($v_{de} = (cT_e/eB_o)L_n^{-1}$) drifts. The solution of the potential equation yields a localizing trapping potential which e-folds away from the trapping region with the characteristic shielding length $\lambda_k = (1 + k_y^2 \rho_s^2 - \omega_{*e}/k_{\parallel} u_{\parallel})^{-1}$. Cross field trapped particle motion is found from the drifts associated with the potential ($v_x = -(c/B_o)\partial\phi/\partial y$, $v_y = (c/B_o)\partial\phi/\partial x$) to be vortical. Carrying out the maximization procedure, the cross field scales Δx and Δy are found to range from a few ρ_s up to a fraction of the system size. The hole depth is proportional to the width in velocity space $-\tilde{f}_k = (\Delta v_{\parallel}/6v_{te}^2)[g(\Delta x/\lambda_k)]^{-1}$, where the width is given by $\Delta v_{\parallel} = (2|e|\phi/m_e)^{1/2}(3/8)^{1/2}\ g(\Delta x/\lambda_k)^{1/2}(1 - \exp(-\Delta x/\lambda_k))^{-1/2} < 1$, and g

is a structure function. The width is such that the trapping criterion $\Delta v_{\parallel} < v_{tr}$ is satisfied explicitly. Thus the entropy maximization constraint is internally consistent with the stipulation that the trapped particle distribution is, in reality, trapped in the self consistent potential.

Drift holes, like clumps, are nonlinearly unstable. The conservation of phase space density

$$\partial/\partial t \int d^3x \int dv_{\parallel} \tilde{f}^2 = -2\partial/\partial t \int d^3x \int dv_{\parallel} \langle f \rangle \tilde{f} \qquad (2)$$

provides for hole growth in response to movement of the hole relative to the background plasma $\langle f \rangle$. When passing ions are accelerated through the hole potential, bulk plasma electrons follow in order to satisfy quasineutrality. Owing to a spatial gradient in x, more ions and electrons move down the gradient than up, placing the hole in a region of greater background plasma density. Conservation of phase space density requires that the hole depth increase as the hole moves into a region of greater $\langle f \rangle$. The growth rate is given by $\gamma = \omega_{*e}(e\phi/T_e)^{1/2} |\mathrm{Im}\chi_i| S(\Delta x/\lambda_k)$ where χ_i is the ion susceptibility and $S(\Delta x/\lambda_k)$ is a structure function of order unity. The presence of the ion susceptibility reflects the role of hole-ion interaction. This scaling is in sharp contrast to linear growth(which scales as the electron susceptibility) and allows holes to grow below the linear threshold. The growth rate, scaling as $\phi^{1/2}$ is manifestly nonlinear in character. Particle excursion during hole growth is limited to Δx, since particles beyond a shielding length do not feel the hole potential. This saturation of growth suggests that mixing length notions might be replaced by the concept of saturation determined by a characteristic scale Δx representing the most probable fluctuation.

Transport and Relaxation

The nonlinear structures we have discussed have a profound effect on transport. This is strikingly illustrated by considering the transport driven by magnetic fluctuations in drift-Alfven turbulence[5]. Two related models are described. The first is concerned with the evolution of an isolated blob in a drift-Alfven system. A paradigm for such an object is a magnetostatic drift hole[6], which is a magnetic flutter analogue of the electrostatic drift hole just described. In the second model, statistical averaging is used to construct a Lenard-Balescu turbulent collision integral for the relaxation of $\langle f \rangle$ due to fully developed drift-Alfven turbulence.

The conservation of phase space density, Eq. (2), describes the evolution of the isolated blob f, and the relaxation of the average distribution $\langle f \rangle$. Expanding $\langle f \rangle$ around x_o ($\langle f \rangle = \langle f(x_o, u_{\parallel}) \rangle + (x-x_o)\partial \langle f \rangle / \partial x |_{x_o, u_{\parallel}}$) and noting that, for drift-Alfven turbulence, $dx/dt = cE_\theta/B_o + v_{\parallel}B_r/B_o$ it follows that

$$\int dv_{\parallel} \int dx \, \partial/\partial t \, \tilde{f}^2 = -2\partial \langle f \rangle / \partial t |_{x_o, u_{\parallel}} \left(\frac{c}{B_o} \langle E_\theta n_e \rangle_b - \frac{\langle B_r J_{\parallel e} \rangle_b}{|c| B_o} \right) , \qquad (3)$$

where $\langle \; \rangle_b$ is the average over the blob volume. Imposing quasineutrality $(n_i = n_e)^b$ the first term on the right hand side of Eq. (3) becomes $c/B_o \langle E_\theta n_i \rangle_b = ck^2/B_o \langle \phi^2 \rangle \mathrm{Im}\chi_i$ reproducing the results of electrostatic hole growth. The flutter contribution to Eq.(3) (second term) is subject to Ampere's law ($J_{\parallel e} = -\nabla_{\perp}^2 A_{\parallel}$, for negligible ion current). Since $B = \nabla A_{\parallel} \times \hat{n}$ and $\nabla \cdot B = 0$, it

follows that $\langle B_r \nabla_\perp^2 A_{\parallel} \rangle_b = -\langle \partial/\partial r (B_r/B_\theta) \rangle_b$ which ultimately contributes only surface terms of $O(\Delta x/L_x) << 1$. Hence, in this simple system, magnetic fluctuations do not result in the evolution of $\tilde{f}$ nor in the relaxation of $\langle f \rangle$. This result may be viewed as a consequence of the self-trapping fields generated by self-bound phase space structures. Alternatively, self-consistency constraints (Ampere's law) ensure that transport driven by blobs is ambipolar over blob scales.

Transport in fully developed drift-Alfven turbulence is governed by an averaged Vlasov equation. The evolution of $\langle f \rangle$ is driven by the radial phase space flux: $\partial \langle f \rangle / \partial t = \partial \Gamma_\Gamma / \partial r$ where

$$\Gamma_\Gamma = \left\langle \frac{c}{B_o} \nabla_y \left(\phi - \frac{v_{\parallel}}{c} A_{\parallel}\right) \hat{h} \right\rangle = \sum_{k,\omega} \mathrm{Re}\left(i \frac{c}{B_o} k_y \left\langle \left(\phi - \frac{v_{\parallel}}{c} A_{\parallel}\right) \hat{h} \right\rangle_{k,\omega} \right) . \quad (4)$$

Here, $\hat{h}$ is the nonadiabatic part of the fluctuating distribution. Including fluctuations $h^{(c)}$ which are phase coherent with the potentials ϕ and $A_{\parallel}$ (collective resonances) and incoherent fluctuations $\tilde{h}$ (clumps or blobs), the right hand side of the averaged Vlasov equation can be represented as a Lenard-Balescu turbulent collision integral. The coherent fluctuations drive (quasilinear) diffusion and the incoherent fluctuations give rise to a collisionless drag. With the imposition of Ampere's law and quasineutrality a cancellation of the diffusion terms by the electron part of the drag terms occurs. Since the ion part of the magnetic drag is proportional to negligible ion current contributions, the transport is governed by the ion part of the electrostatic drag:

$$\Gamma_\Gamma = \sum_{k,\omega} \frac{ck_y}{B_o |k_{\parallel}|} 2\pi \, \delta(\phi - k_{\parallel} u_{\parallel}) \, \mathrm{Re}\left(\mathcal{L}^{-1}_{k,\omega} \langle \phi \tilde{h} \rangle \, d^{A,A}_{k,\omega} \, \mathrm{Im} d^{\phi,\phi}_{k,\omega(\mathrm{ion})} \right) \quad (5)$$

where $\mathcal{L}^{-1}$ is the inverse eigenfunction operator and the d's are dielectric tensor elements. This result is analogous to those obtained using Lenard-Balescu equations for a 1-D electron-ion plasma. In that system, constraints of momentum and energy conservation on the interaction of localized phase space fluctuations preclude momentum exchange in like-particle collisions, thus preventing relaxation of $\langle f \rangle$.

Both the isolated blob model and the fully developed turbulence model indicate that electrostatic fluctuations alone produce transport in drift-Alfven turbulence. This conclusion effectively underscores the critical role played by incoherent fluctuations in turbulence and argues for the necessity of their inclusion in plasma turbulence models.

References

1. S.J. Zweben, Phys. Fluids 28, 974(1985).
2. T.H. Dupree, Phys. Fluids 15, 334(1972).
3. P.W. Terry and P.H. Diamond, in *Statistical Physics and Chaos in Fusion Plasmas*, ed. by W. Horton and L. Reichl (Wiley, New York, 1984) p. 335.
4. T.H. Dupree, Phys. Fluids 25, 277(1982).
5. P.W. Terry, P.H. Diamond, and T.S. Hahm, Institute for Fusion Studies Report #IFS203, 1985.
6. P.W. Terry, et al., Bull. Amer. Phys. Soc. 30, 1512(1985).